ARTICLE

BIOTECHNOLOGY AND BIOENGINEERING WILEY

# Modeling the impact of amino acid substitution in a monoclonal antibody on cation exchange chromatography

David Saleh[1,2] | Rudger Hess[1,2] | Michelle Ahlers-Hesse[1] | Nicole Beckert[3] | Markus Schönberger[1] | Federico Rischawy[1,2] | Gang Wang[1] | Joschka Bauer[3] | Michaela Blech[3] | Simon Kluters[1] | Joey Studts[1] | Jürgen Hubbuch[2]

[1]Late Stage DSP Development, Boehringer Ingelheim, Biberach, Germany

[2]Institute of Engineering in Life Sciences, Section IV: Biomolecular Separation Engineering, Karlsruhe Institute of Technology (KIT), Karlsruhe, Germany

[3]Pharmaceutical Development Biologics, Boehringer Ingelheim, Biberach, Germany

**Correspondence**
Jürgen Hubbuch, Institute of Engineering in Life Sciences, Section IV: Biomolecular Separation Engineering, Karlsruhe Institute of Technology (KIT), Fritz-Haber-Weg 2, 76131 Karlsruhe, Germany.
Email: juergen.hubbuch@kit.edu

## Abstract

A vital part of biopharmaceutical research is decision making around which lead candidate should be progressed in early-phase development. When multiple antibody candidates show similar biological activity, developability aspects are taken into account to ease the challenges of manufacturing the potential drug candidate. While current strategies for developability assessment mainly focus on drug product stability, only limited information is available on how antibody candidates with minimal differences in their primary structure behave during downstream processing. With increasing time-to-market pressure and an abundance of monoclonal antibodies (mAbs) in development pipelines, developability assessments should also consider the ability of mAbs to integrate into the downstream platform. This study investigates the influence of amino acid substitutions in the complementarity-determining region (CDR) of a full-length IgG1 mAb on the elution behavior in preparative cation exchange chromatography. Single amino acid substitutions within the investigated mAb resulted in an additional positive charge in the light chain (L) and heavy chain (H) CDR, respectively. The mAb variants showed an increased retention volume in linear gradient elution compared with the wild-type antibody. Furthermore, the substitution of tryptophan with lysine in the H-CDR3 increased charge heterogeneity of the product. A multiscale in silico analysis, consisting of homology modeling, protein surface analysis, and mechanistic chromatography modeling increased understanding of the adsorption mechanism. The results reveal the potential effects of lead optimization during antibody drug discovery on downstream processing.

**KEYWORDS**
antibody purification, cation exchange chromatography, developability assessment, mechanistic chromatography modeling, protein surface analysis

---

# 1 | INTRODUCTION

In recent years, the number of monoclonal antibodies (mAbs) investigated in clinical studies has steadily increased (Kaplon et al., 2020; Kaplon & Reichert, 2019). Manufacturing and material supply for preclinical and clinical trials form a major building block in biopharmaceutical product development and is often referred to as chemistry, manufacturing, and controls (CMC). A recent cost evaluation performed by Farid et al. (2020) predicted that CMC activities represent 13%–17% of the total R&D budget from preclinical trials to regulatory approval. Their calculation considered costs caused by ~92% of candidates that fail during preclinical and clinical development (Farid et al., 2020). Biopharmaceutical organizations strive to streamline development by using computer-aided sequence optimization tools in drug discovery that increase the likelihood of successful CMC programs within a strict timeframe (Bailly et al., 2020; Bauer et al., 2020; van der Kant et al., 2017). Current strategies for developability assessment rely on in silico techniques to predict aggregation propensities, solubility issues, or long-term stability of the mAb product (Bauer et al., 2020; Seeliger et al., 2015). Compared with stability aspects in formulation development, how single amino acid substitutions in lead candidates may affect developability of the downstream process (DSP) is poorly understood.

Industrial DSP of biopharmaceuticals relies heavily on chromatographic separation techniques. For the purification of mAbs, preparative cation exchange (CEX) chromatography is frequently employed as a polishing step (H. F. Liu et al., 2010; Shukla et al., 2007). CEX chromatography allows the removal of process-related impurities, including DNA, host cell proteins, endotoxins, or leached Protein A (H. F. Liu et al., 2010, 2011). Due to its high selectivity toward protein charge, CEX chromatography can also separate an antibody from its product-related impurities, for example, size or charge variants. Despite the favorable properties regarding impurity removal, CEX chromatography remains one of the most development-intensive unit operations in the DSP. The comparably strong effect of a mAb's structural characteristics on elution behavior in CEX chromatography demands an adaption of process conditions for each product. Therefore, a significant body of research has focused on understanding the relationship between protein structure properties and adsorption behavior. Adsorption in protein chromatography can be investigated using molecular dynamic simulations (Dismer & Hubbuch, 2010; Lang et al., 2015). Monte Carlo simulations performed by Zhou et al. (2004) showed that antibodies tend to have a "head-on" fragment antibody $(F_{ab})_2$ binding orientation on negatively charged surfaces and an "end-on" fragment crystallizable ($F_c$) binding orientation on positively charged surfaces, at high surface charge density and low salt concentration. In multimodal (MM) systems, the chromatographic behavior and binding orientation of model proteins (Banerjee et al., 2017; Freed et al., 2011; Woo et al., 2015) and mAbs (J. Robinson et al., 2018) depends on ligand structure and surface properties of the molecule. Furthermore, J. Robinson et al. (2020) showed that the domain contribution of mAbs in MM chromatography is affected by the mobile phase pH value.

In contrast to qualitative analysis, quantitative structure–property relationship (QSPR) models correlate structural descriptors with chromatographic behavior by applying mathematical models. QSPRs based on the crystal structure of non-mAb proteins allowed the prediction of protein retention times (Mazza et al., 2001) and adsorption isotherm parameters (Ladiwala et al., 2005) in ion-exchange (IEX) chromatography. J. R. Robinson et al. (2017) applied QSPR modeling to the purification of homologous $F_{ab}$ variants on MM resins. Kittelmann et al. introduced an orientation sensitive QSPR approach for model proteins (Kittelmann et al., 2017a) and mAbs (Kittelmann et al., 2017b) in IEX chromatography. A comprehensive study performed by Ishihara et al. (2005) investigated the elution behavior of 28 mAbs in Protein A affinity and CEX chromatography. For CEX chromatography, the salt concentrations at peak maximum correlated with the surface positive charge distribution of the heavy chain variable region (Ishihara et al., 2005). To the best of our knowledge, results on how substituting residues within the adsorption relevant surface of a full-length mAb would influence CEX chromatography have not been published yet.

In contrast to structure-based modeling techniques, mechanistic models describe the physical effects in chromatography columns on a macroscopic level. During the last years, mechanistic chromatography modeling became a state-of-the-art technology in biopharmaceutical DSP development. Possible applications of mechanistic models are process optimization (Hahn et al., 2014; Huuk et al., 2014), model-guided scale-up (Benner et al., 2019; Mollerup et al., 2007), in silico robustness analysis (Close et al., 2014; Jakobsson et al., 2007; Rischawy et al., 2019), or root cause investigation (Wang et al., 2017). The process understanding provided by mechanistic chromatography models enables in silico DSP development in line with the Quality by Design (QbD) concept (Mollerup et al., 2008). Chromatography models consist of partial differential equations describing mass transport and protein adsorption phenomena. For IEX chromatography, the adsorption can be modeled using the stoichiometric displacement model (SDM) (Boardman & Partridge, 1955). The SDM is based on the electrostatic equilibrium theory and formulates the multipoint binding of proteins under consideration of displacement effects. Brooks and Cramer (1992) extended the SDM toward the steric mass-action (SMA) model to cover the shielding effects of bound protein on the resin surface.

Previous work has demonstrated the predictive power of SMA models, even when extrapolating beyond the experimental conditions applied for model calibration (Briskot et al., 2019). Despite the proven predictive power and the mechanistic nature of the SMA model, it is not clear which structural characteristics of mAbs influence adsorption model parameters. For example, Rüdt et al. (2015) built an SDM model for an $F_c$ fusion protein and corresponding aggregates by assuming constant characteristic charge values for both protein species. Other authors (Borg et al., 2014; Briskot et al., 2019) reported differing characteristic charge parameters for mAb size and charge variant, due to altering numbers of charged groups interacting with the resin. Furthermore, it is unclear if steric shielding is exclusively a function of the chromatographic ligands blocked by the adsorbed protein or if it further considers non-adsorptive or repulsive effects (Ladiwala et al., 2005). Due to the missing

correlations between adsorption isotherm parameters and structural characteristics of multidomain proteins such as mAbs, the preferred practice for model calibration often involves curve fitting to experimental data (Briskot et al., 2019; Hahn, Huuk, et al., 2016). Substitution of single charged amino-acid side chains in the adsorption relevant region of full-length mAbs could elucidate the correlations between protein structure and macroscopic adsorption model parameters.

The aim of the present work is to gain a deeper understanding of the binding mechanism of mAbs in preparative CEX chromatography. Therefore, multiple purification experiments were performed for a full-length IgG1 mAb, and two variants differing in a single amino acid within the complementarity-determining region (CDR). An additional positive charge in the L- and H-CDR of the mutated mAbs increased their retention volume during linear salt gradient elution (LGE). Potential effects of amino acid substitutions on the developability of the CEX unit operation were investigated in chromatography runs at low and high loading densities. Homology modeling and protein surface analysis identified exposed mAb regions that mediate the adsorption process. The data set enabled the estimation of SMA model parameters for the three mAbs. The identified effects of amino acid substitutions on adsorption model parameters could support model calibration and QSPR modeling.

## 2 | METHODS

### 2.1 | Process conditions and mAbs

The mAb polishing step was performed on the strong CEX resin POROS XS (Thermo Fisher Scientific). Column-specific parameters and the equations used for their calculation are listed in Table 1. Tracer injections with blue dextran and 1 M sodium chloride (both from Sigma-Aldrich) enabled the calculation of the interstitial volume, $V_{int}$ and total liquid volume, $V_t$, respectively. The ionic capacity $\Lambda$ was determined by acid–base-titration (Huuk et al., 2016). Column characterization experiments were conducted as triplicates. Chemicals used in this study were

of pharmaceutical grade. All buffers were prepared with deionized water and filtered with a 0.2-μm sterile filter. Column experiments were performed on the preparative chromatography system ÄKTA Avant 25 controlled via Unicorn 7 (both from Cytiva). Sodium acetate buffer at pH 5.25 was used for all preparative CEX experiments. The column was equilibrated at pH 5.25 and a counterion concentration of 0.05 M sodium. Buffer exchange of protein samples into the equilibration buffer resulted in defined loading conditions. During gradient elution, counterion concentration increased from 0.05 to 0.50 M sodium. The loading density was 1 g/$L_{Resin}$ for LGEs in the linear region of the adsorption isotherm and 30 g/$L_{Resin}$ for high loading density runs. Samples applied for low and high loading experiments had protein concentrations of 1 and 3 g/L, respectively. Loading densities were adjusted via the applied sample volume, considering the 10.68 ml column volume. 1 and 0.1 M sodium hydroxide were used for column regeneration and storage, respectively.

The three model proteins used in this study are IgG1 mAbs expressed in Chinese hamster ovary cells (Boehringer Ingelheim Pharma GmbH & Co. KG). The mAbs were captured via Protein A affinity chromatography. Two mutants (M1 and M2) with additional positively charged groups in the CDRs were derived from a corresponding wild-type (WT) antibody. Surface charge of M1 was increased by substitution of serine with lysine in the L-CDR3. For M2, a tryptophan in the H-CDR3, was substituted with lysine. The amino acid substitutions were introduced to affect the biophysical properties of the mAb via modification of surface-exposed hydrophobic and charged patches. This methodology can reveal the possible effects of mAb lead optimization on CMC properties in upstream, downstream, and formulation development.

### 2.2 | Homology modeling and protein surface analysis

Full-length homology models of investigated mAbs were built in Maestro BioLuminate 3.7 (Schrödinger) following the method

**TABLE 1** Experimentally determined system- and column-specific model parameters

| Parameter | Symbol | Value | Unit | Equation | References |
|---|---|---|---|---|---|
| Length | $L$ | 136 | mm | - | - |
| Diameter | $d$ | 10 | mm | - | - |
| Column volume | $V$ | 10.68 | ml | $V = \pi \frac{d^2}{4} L$ | - |
| Bead radius | $r_p$ | 25 | μm | - | - |
| Interstitial porosity | $\varepsilon_{col}$ | 0.41 | - | $\varepsilon_{col} = \frac{V_{int}}{V}$ | Hahn, Huuk, et al. (2016) |
| Total porosity | $\varepsilon_t$ | 0.78 | - | $\varepsilon_t = \frac{V_t}{V}$ | Hahn, Huuk, et al. (2016) |
| Particle porosity | $\varepsilon_p$ | 0.63 | - | $\varepsilon_p = \frac{V_t - V_{int}}{V - V_{int}}$ | Hahn, Huuk, et al. (2016) |
| Axial dispersion | $D_{ax}$ | 0.14 | mm²/s | $D_{ax} = \frac{u L s_{NaCl}^2}{(2 V_t)^2}$ | Hunt et al. (2017) |
| Ionic capacity | $\Lambda$ | 0.49 | M | $\Lambda = \frac{c_{NaOH} V_{NaOH}}{V(1 - \varepsilon_t)}$ | Hahn, Huuk, et al. (2016); Huuk et al. (2016) |

developed by Zhu et al. (2014). Separate templates for light and heavy chains were selected based on the sequence identity of framework regions. For WT, M1, M2, the framework region templates were 3SO3 and 3T2N (PDB accession codes) for heavy and light chains, respectively. Comparably low sequence identity (<40%) between available templates and the 14 residues long H-CDR3 demanded an ab initio structure prediction using the Prime method (Zhu & Day, 2013). Following the method developed by Zhu et al. (2014), all structures were prepared accordingly before starting loop prediction. Structure preparation included the assignment of polar hydrogen positions, protonation states, and energy minimization using the OPLS3e force field (Roos et al., 2019). Surface patches and protein descriptors were calculated within BioLuminate, at pH 5.25 (Olsson et al., 2011; Sankar, Krystek, et al., 2018).

## 2.3 | Mechanistic chromatography modeling

The simulation software ChromX (GoSilico GmbH) was used for mechanistic chromatography modeling. The transport dispersive model in Equation (1) was applied as a column model (Baumann et al., 2015; Hahn, Huuk, et al., 2016). In Equation (1), the change of the concentration $c_i(x, t)$ is a function of the convective mass transport in the interstitial volume of the packed bed with the superficial velocity $u$. Furthermore, the model considers axial dispersion $D_{ax}$ effects and interfacial mass transfer between the interstitial volume defined by the bed porosity $\varepsilon_{col}$ and the particle pores. Film diffusion effects in the particle boundary layer and pore diffusion in the particle phase are expressed by the effective mass transfer parameter $k_{eff, i}$. Equation (2) represents the accumulation of mass in the pore volume $c_i$ and the stationary phase $q_i$. Danckwerts' boundary conditions are given in Equations (3) and (4).

$$\frac{\partial c_i(x, t)}{\partial t} = -\frac{u}{\varepsilon_{col}} \frac{\partial c_i(x, t)}{\partial x} + D_{ax} \frac{\partial^2 c_i(x, t)}{\partial x^2}$$
$$- \frac{(1 - \varepsilon_{col})}{\varepsilon_{col}} \left( \frac{3}{r_p} k_{eff,i} \left( c_i(x, t) - c_{p,i}(x, t) \right) \right), \quad (1)$$

$$\frac{\partial c_{p,i}(x, t)}{\partial t} = \frac{3}{r_p} \frac{k_{eff,i}}{\varepsilon_p} \left( c_i(x, t) - c_{p,i}(x, t) \right) - \frac{1 - \varepsilon_p}{\varepsilon_p} \frac{\partial q_i(x, t)}{\partial t}, \quad (2)$$

$$\frac{\partial c_i}{\partial x}(0, t) = \frac{u(t)}{\varepsilon_{col} D_{ax}} (c_i(0, t) - c_{in,i}(t)), \quad (3)$$

$$\frac{\partial c_i}{\partial x}(L, t) = 0. \quad (4)$$

Protein adsorption is modeled using the SMA isotherm (Brooks & Cramer, 1992). Equation (5) shows the kinetic form of the SMA isotherm modified by Hahn, Baumann, et al. (2016), where $q_i$ and $c_{p, i}$ denote the protein concentration in the solid and liquid phase of the particle, respectively. The SMA model formulates the equilibrium binding behavior of the protein considering the salt concentration in the pore phase $c_s$, the ionic capacity of the resin $\Lambda$ and protein-specific model parameters. The protein characteristic charge $\nu_i$ accounts for the number of charges interacting with the resin, while

steric shielding $\sigma_i$ considers the number of functional groups on the resin blocked by the protein due to steric hindrance. Additionally, the constants $k_{eq, i} = k_{ads, i}/k_{des, i}$, and $k_{kin, i} = 1/k_{des, i}$ comprise adsorption and desorption rates of the modeled proteins.

$$k_{kin,i} \frac{\partial q_i}{\partial t} = k_{eq,i} \left( \Lambda - \sum_{j=1}^{k} (\nu_j + \sigma_j) q_j \right)^{\nu_i} c_{p,i} - q_i c_s^{\nu_i}, \quad (5)$$

$$q_{salt} = \Lambda - \sum_{j=1}^{k} \nu_j q_j. \quad (6)$$

Estimation of protein-specific model parameters is the first step, before a mechanistic model can be applied to real-world tasks in DSP development. The Yamamoto method enabled the analytical solution of $\nu_i$ and $k_{eq, i}$ using a set of LGEs at differing salt gradient slopes. Equation (7) describes the linear relationship between the normalized gradient slope $GH$ and the elution salt concentration $c_{s, i}$ of component $i$ at diluted loading conditions (Ishihara et al., 2005; Osberghaus et al., 2012; Rüdt et al., 2015; Yamamoto et al., 1987; Yamamoto et al., 1988). Equations (8) and (9) lead to the calculation of the normalized gradient slope $GH$, where $c_{s, initial}$ is the salt concentration at the gradient begin, $c_{s, final}$ is the salt concentration at the gradient end, and $V_G$ is the gradient length in milliliters. The isotherm parameters defining the nonlinear region of the SMA isotherm, $k_{kin, i}$ and $\sigma_i$, were estimated using the inverse method developed by Hahn, Baumann, et al. (2016) and Hahn, Huuk, et al. (2016).

$$log(GH) = (\nu_i + 1) log(c_{s,i}) - log(k_{eq,i} \Lambda^{\nu_i} (\nu_i + 1)), \quad (7)$$

$$g = \frac{c_{s,final} - c_{s,initial}}{V_G}, \quad (8)$$

$$GH = g(V_{col} - \varepsilon_t V_{col}). \quad (9)$$

## 3 | RESULTS

### 3.1 | Process behavior and protein surface analysis

The aim of the present study was to analyze the effects of single amino acid substitutions in the CDR of an mAb on process behavior in CEX chromatography. The two mutants M1 and M2 had an additional positively charged group in the CDR compared with the WT mAb. Details on amino acid substitutions are given in Section 2.1. An identical set of preparative CEX experiments was performed for three mAb variants. In this section, the results of LGE experiments under low loading conditions (1 g/L_Resin) are compared to the in silico analysis of corresponding homology models. Figure 1d,f show LGE experiments at a gradient length of 20 column volumes (CV) and mobile phase pH 5.25. The WT antibody eluted first, followed by the mutants M1 and M2 with additional positively charged amino acid side chains in the CDR. WT, M1, and M2 eluted at a sodium counter-ion concentration of 0.336, 0.416, and 0.433 M during salt gradient elution, respectively. Besides the delayed retention volume, similar
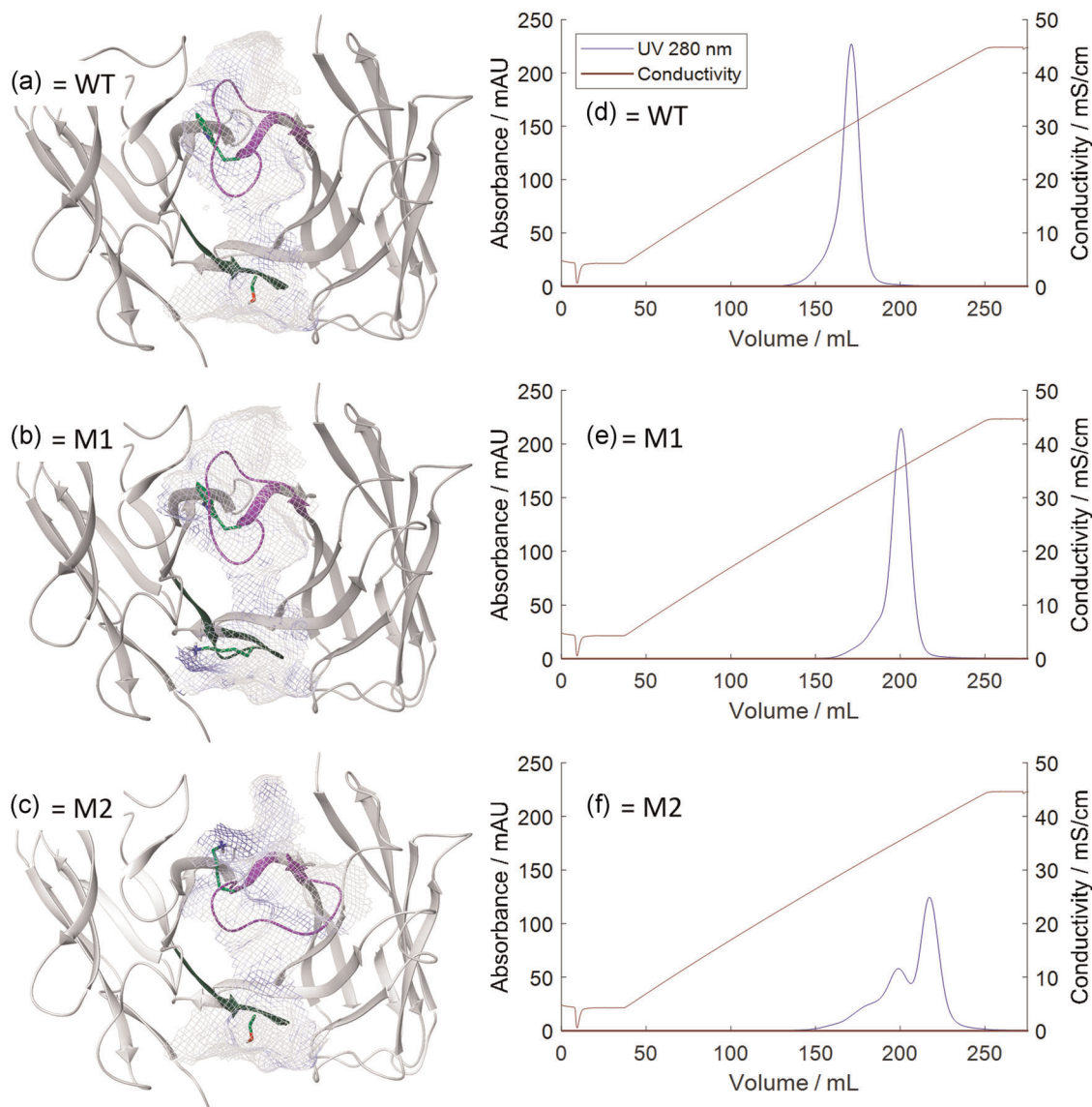
**FIGURE 1** Protein surface analysis and elution behavior in cation-exchange (CEX) chromatography at 1 g/L$_{Resin}$ loading density. Predicted Fv homology models: (a) wild type (WT) with tryptophan in the heavy chain (HC) and serine in the light chain (LC); (b) M1 with tryptophan in HC and lysine in LC; (c) M2 with lysine in HC and serine in LC. The solvent-exposed surface is shown as mesh, and positively charged patches close to H-CDR3 (purple) and L-CDR3 (dark green) are marked in blue. (d–f) Respective CEX chromatograms of linear salt gradient elution experiments conducted on POROS XS at pH 5.25, with 20 column volume gradient length, and a flow velocity of 200 cm/h [Color figure can be viewed at wileyonlinelibrary.com]

peak shapes could be observed for the WT and M1. In contrast, M2 showed an increased elution pool volume compared to WT and M1, caused by a distinct pre-peak with shoulder. Results of analytical chromatography (HP-CEX) indicated that the pre-peak of M2 was caused by an increased charge heterogeneity of the loading material (data not shown).

The visible effect of point mutations in the CDRs on the elution behavior during CEX chromatography demanded a thorough investigation of structural characteristics causing these phenomena. Homology models were calculated for the three IgG1 mAbs using the workflow described in Section 2.2. Antibody structure predictions in Figure 1a–c confirmed that the substituted side chain residues were

solvent-exposed. Due to identical F$_c$ regions, protein surface analysis was performed for the F$_{ab}$ only, while the pI and net charge calculations were based on full-length homology models. Table 2 compares pI values obtained via capillary isoelectric focusing (cIEF) with in silico predicted pI values and protein descriptors. Both, in silico and wet-lab experiments, could not measure significant differences between pI values of the three mutants. Model-based net charge of the full-length IgG1 mutants at pH 5.25 increased to 50 from 48. The number of positive charges per CDR increased to 7 from 6 for the mutated mAbs at pH 5.25. Additionally, compared with WT, point mutations increased the sum energy of positive surface patches larger than 30 Å$^2$ in the CDRs by 20% and 28% for M1 and M2,

**TABLE 2** Molecular descriptors and pI values obtained via in silico prediction and cIEF measurements

| | pI[a] (−) | pI (−) | Net charge[a] | Formal charge CDR[a] | Positive patch energy CDR[a] (kcal/mol) |
|---|---|---|---|---|---|
| Method | **In silico** | cIEF | In silico | In silico | In silico |
| WT | 9.2 | 8.9 | 48 | 6 | 499 |
| M1 | 9.2 | 8.9 | 50 | 7 | 599 |
| M2 | 9.2 | 8.9 | 50 | 7 | 638 |

Abbreviations: CDR, complementarity-determining region; cIEF, capillary isoelectric focusing; WT, wild type.

[a]In silico descriptors were calculated based on homology models at pH 5.25.

**TABLE 3** SMA isotherm parameters of WT, M1, and M2 at pH 5.25 on POROS XS

| | $v_i$ (−) | $k_{eq,i}$ (−) | $k_{kin,i}$ (sM$^v$) | $\sigma_i$ (−) |
|---|---|---|---|---|
| WT | 11.7 | 0.08 | 4.58E−05 | 53 |
| M1 | 11.6 | 0.65 | 3.41E−04 | 51 |
| M2 Main | 11.9 | 1.82 | 4.09E−04 | 38 |
| M2 APG1 | 11.3 | 0.65 | 1.05E−04 | 38 |
| M2 APG2 | 11.3 | 0.15 | 2.74E−04 | 38 |

Note: Acidic charge variants of M2 were lumped in two APG based on their retention time in preparative chromatography.

Abbreviations: APG, acidic peak group; SMA, steric mass-action; WT, wild type.

respectively. Protein surface analysis in Figure 1 visualizes the additional positively charged patches in the CDR of mutated mAbs. Due to the high degree of solvent exposure, all depicted surface patches could potentially be involved in the adsorption process. For M1, serine was substituted with lysine, adding a positive patch in a neutral region of the WT mAb. Besides the differences in positive surface charges, ab initio H-CDR3 loop prediction via the Prime method (Zhu & Day, 2013) resulted in similar conformations for WT and M1. In contrast, the substitution of tryptophan with lysine in M2 influenced the predicted conformation of the H-CDR3, increasing solvent exposure compared with WT and M1.

## 3.2 | Chromatography modeling

Homology modeling and protein surface analysis provided insights into the structural properties of the mAbs leading to differences in their chromatographic behavior. Mechanistic chromatography modeling aims to increase process understanding on a macroscopic level by describing the physical effects in the chromatographic system. This section investigates the effects of changes in the protein structure on macroscopic adsorption model parameters.

System and column characterization were crucial for the following estimation of protein-specific model parameters. All results and respective methods of column characterization and are listed in Table 1. POROS XS is a perfusion resin, with comparably low mass transfer resistance. Therefore, $k_{eff,salt}$ was approximated with $r_P/3 = 0.0083$ mm/s (Rodrigues, 1997). For the protein species, the penetration correlation (Guiochon et al., 2006) enabled the calculation of effective mass transfer parameters $k_{eff,i}$ depending on the hydrodynamic radii of the mAbs and the linear flow rate. Identical hydrodynamic radii of 73 Å were computed based on full-length homology models resulting in a $k_{eff,i}$ of 0.0013 mm/s for WT, M1, and M2. Predictions of the height and width of elution peaks at low loading conditions validated assumptions regarding the mass transfer of protein.

Multiple lab-scale experiments for each mAb allowed the estimation of SMA model parameters. Table 3 summarizes the resulting

isotherm parameters. Five LGE experiments were conducted at 1 g/L$_{Resin}$ loading density and altering gradient lengths between 10 and 30 CV. At each gradient slope, the WT eluted first followed by M1 and M2. Figure 2 visualizes the Yamamoto correlation (Equation 7), which enabled the analytical solution of the characteristic charge $v_i$ and equilibrium constant $k_{eq,i}$ based on the five LGE experiments per mAb. The parallel regression lines in Figure 2 resulted in comparable characteristic charge $v_i$. In addition, the predicted and measured net charges and pI values of the homology models in Table 2 did not show a considerable difference between the molecules. In contrast to $v_i$, the equilibrium constants $k_{eq,i}$ of the mutants M1 and M2 in Table 3 increased to approximately 8- and 23-fold compared with the WT, respectively. The characteristic charge $v_i$ and the equilibrium constant $k_{eq,i}$ have a similar effect on the retention volume during LGE elution at low loading densities. Thus, the equilibrium constant $k_{eq,i}$ was the parameter affected by the addition of positively charged groups in the CDR and caused the shifts in retention volume.

Steric shielding $\sigma_i$ and kinetic $k_{kin,i}$, the remaining model parameters defining the nonlinear region of the SMA isotherm, were estimated using the inverse method introduced by Hahn, Baumann, et al. (2016). Here, the model output was fitted to the UV signal at 280 nm wavelength of the high load LGE runs in Figure 3. Similar to $k_{eq,i}$, the kinetic parameter $k_{kin,i}$ increased for the mutated mAbs. The shielding parameters in Table 3 show that the substitution of tryptophan with lysine in M2 reduced $\sigma_i$ by 28% compared with the WT. The single protein species defined for WT and M1 was able to describe peak shapes and retention volumes at 30 g/L$_{Resin}$ loading density. For M2, the increased concentration of acidic charge variants demanded the consideration of additional protein species. Two acidic peak groups (APG1 and APG2) of M2 were defined based on the peak-to-peak ratios measured at the low loading density LGE experiments. The relative input composition of M2 main, M2 APG1, and M2 APG2 was 67%, 16%, and 17%, respectively. Single amino acid substitutions could not affect the characteristic charge parameters of WT, M1, and M2 in a magnitude that would describe the differences in retention volume. Thus, the characteristic charge $v_i$ of the M2 charge variants, APG1 and APG2, was assumed to be equal to the characteristic charge of the M2 main species.
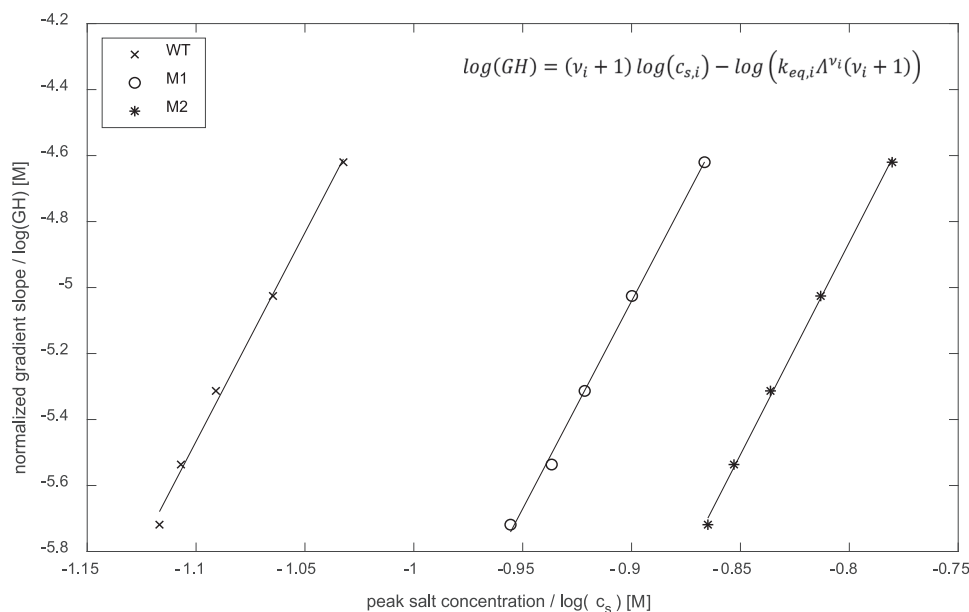
**FIGURE 2** Model calibration for the linear region of the steric mass-action isotherm. Yamamoto method for linear salt gradient elution experiments with 10, 15, 20, 25, 30 column volume gradient length at pH 5.25 on the strong cation exchange media POROS XS. Slope and intercept of linear regressions enabled the calculation of characteristic $v_i$ and $k_{eq,i}$ equilibrium constant, respectively. $R^2 > 0.98$ for all linear regressions

For all three molecules, the transport-dispersive SMA model could describe the UV signal. This indicates that the selected model captured relevant physical effects within the chromatographic system. The comparison of isotherm parameters in Table 3 with structural descriptors in Table 2 shows that macroscopic adsorption model parameters are directly affected by single amino acid substitutions and the resulting protein structure. Besides, the identified effects on mechanistic model parameters, amino acid substitutions influenced process performance at both, low- and high-loading densities. Retention times, charge heterogeneity, and elution pool volumes in preparative column experiments differed between the three mAb variants. Thus, lead optimization can potentially affect preparative purification using CEX chromatography.

## 4 | DISCUSSION

During the last years, a significant body of research has focused on the development of in silico tools for the reduction of aggregation propensity, improvement of solution properties, and optimization of biological activity of therapeutic mAbs (Bauer et al., 2020; Kumar et al., 2018; van der Kant et al., 2017). Optimization of protein stability has been shown to be associated with additional favorable CMC properties, for example, increased expression titers during upstream processing (Bauer et al., 2020; van der Kant et al., 2017). The present study aimed to investigate the effects of single amino acid substitutions in full-length mAbs on the process behavior during preparative CEX chromatography.

Previous work indicated that mAbs bind with their $F_{ab}$ first to strong CEX media (Ishihara et al., 2005; Zhou et al., 2004). In this study, modification of CDR residues that contribute to positive patches on the mAb surface proved the vital role of the $F_{ab}$ and CDR in antibody adsorption on strong CEX media. An identical set of preparative CEX experiments with three mAb variants differing in a single amino acid showed a correlation between the sum positive patch energy of the CDR and retention time during gradient elution. Independent of CDR loop confirmations, the substitution of tryptophan with lysine in the H-CDR3 of M2 increased the elution salt concentration by 32%. This resulted in comparably high salt concentrations in the product pool. The final salt concentration in the product pool needs to be considered in designing the process sequence, when combining CEX with other chromatographic modalities for mAb polishing. Thus, the exchange of a single charged amino acid during lead optimization has the potential to affect resin selection and process design during downstream processing. Despite differences in patch energies and CEX retention times, pI values and net charges of the homology model did not differ significantly between investigated mAbs. While this may seem trivial due to the minimal variation in primary structure, it is important to notice that the experimental pI value is often considered as initial binding strength indicator for the development of IEX chromatography processes. Previous studies could show that solvent-exposed charges on the mAb surface are relevant for protein adsorption in IEX and mixed-mode chromatography (Gudhka et al., 2020; Ishihara et al., 2005; J. Robinson et al., 2018). In this study, targeted amino-acid substitutions within the protein–resin interaction surface emphasized that inhomogeneous charge distribution affects chromatographic
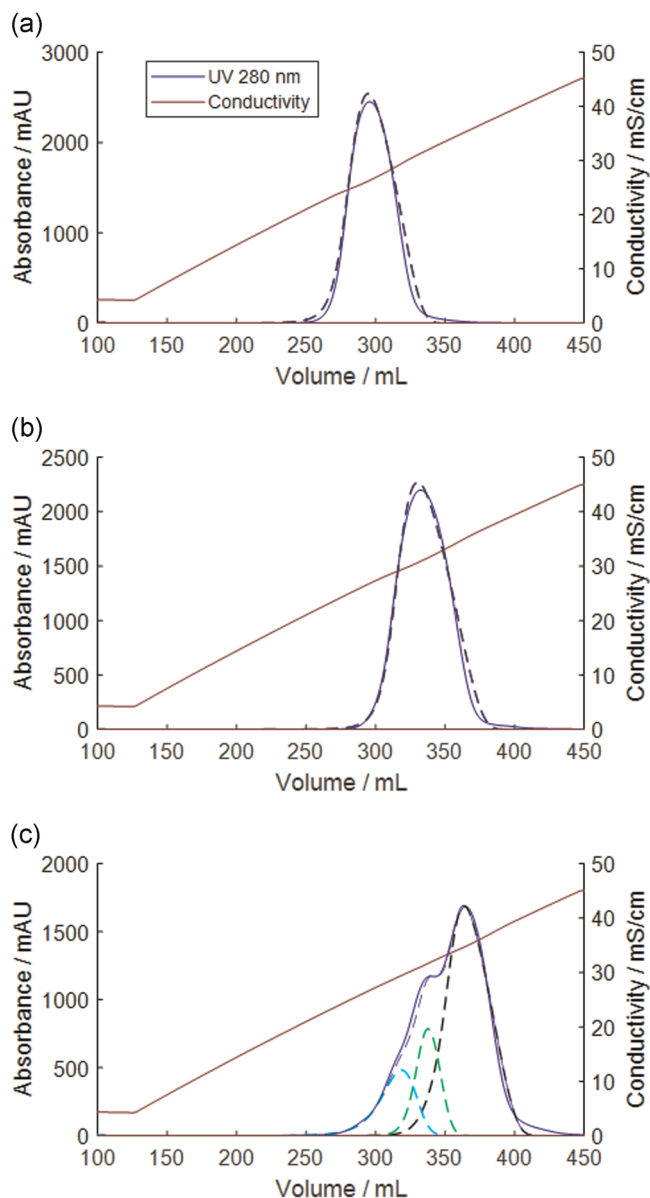
(a)



(b)



(c)



**FIGURE 3** Comparison of simulated and measured chromatograms of the cation exchange process under nonlinear loading conditions. Linear salt gradient elution experiments on POROS XS at 30 g/L$_{Resin}$ loading density, with 30 CV gradient length, and a flow velocity of 200 cm/h. The blue dashed lines indicate simulated sum signals. Solid lines represent experimental data. (a) WT; (b) M1. For WT and M1, a single protein species was simulated. (c) M2. Three protein species were considered in the simulation of the M2 process. Green and cyan dashed lines are simulations of acidic charge variants of M2 [Color figure can be viewed at wileyonlinelibrary.com]

behavior of proteins with almost identical net charges. Therefore, local and global molecule properties should be considered equally in the design of IEX chromatography processes, especially for large multidomain molecules such as mAbs. Nonetheless, the unraveled correlations and binding orientation are only valid for the investigated strong CEX media. In contrast to our data, Müller-Späth

et al. (2008) separated mAbs with differing numbers of C-terminal lysine using an analytical weak CEX media at pH 6.3. Their data suggests that the F$_c$ part of mAbs contributes to protein adsorption on weak CEX media. Consequently, protein adsorption is equally dependent on the molecule structure and the chromatographic ligand. Future studies are required to shed light on the correlations between antibody structure and process behavior in other chromatographic unit operations.

Besides the shift in retention volume, the substitution of tryptophan with lysine in the H-CDR3 of M2 had a significant effect on the percentage of acidic charge variants and the resulting elution profiles in Figures 1 and 3. Interestingly, ab initio H-CDR3 structure prediction using Prime method (Zhu & Day, 2013) resulted in an increased solvent exposure of the M2 H-CDR3 compared with the WT and M1 mAbs (Figure 1). Recently, Lan et al. (2020) reported an anomalous charge variant profile of an IgG1 mAb in analytical CEX chromatography caused by two discrete conformational states of the H-CDR3. Their analytical and molecular modeling investigation revealed a pH-dependent equilibrium between "open" and "closed" conformational states of the H-CDR3. Furthermore, their work identified a neighboring tryptophan residue in the LC showing reduced solvent exposure at lower pH values. Previous work underlined that aromatic and hydrophobic groups have a stabilizing effect on CDR loop conformation (van der Kant et al., 2019). Therefore, it can be assumed that the substitution of tryptophan with lysine in M2 destabilized the energetically favored loop conformation and increased solvent exposure of the H-CDR3 (Figure 1). Charge heterogeneity is a common feature of therapeutic mAbs, which does not necessarily influence their efficacy (Lan et al., 2020; H. Liu et al., 2008). However, when comparing the results to previous work (Saleh et al., 2020), the distinct peak shoulder in the chromatograms of M2 is uncommon for IgG1 mAbs in preparative CEX chromatography. When applying identical UV-based collection criteria to the three mAb variants, the elution pool volume of M2 increases by ~33% compared with WT and M1. Due to limited tank capacities in manufacturing facilities and processing time related to the subsequent product concentration via ultrafiltration/diafiltration, the high elution pool volume represents an undesired CMC property. Hence, the substitution of potentially stabilizing, aromatic groups within the H-CDR3 should be avoided during lead optimization. Based on these findings, mAb candidates with favorable CMC properties can be selected for a streamlined process development. Alternatively, a qualitative prediction of protein adsorption based on the sequence may allow an early estimation of experimental efforts necessary for developing polishing chromatography. In case an mAb shows a high likelihood for unfavorable CMC properties in CEX chromatography, for example, increased elution pool volumes or high salt concentration in the elution pool, a broad resin screening with differing chromatographic modalities can be planned early during process development. For a holistic DSP developability assessment, additional unit operations should be added to the multiscale modeling workflow. However, our results indicate that CEX chromatography is sensitive to minimal changes in the primary structure of

—WILEY—

mAbs. For other unit operations in common DSP platforms, for example, filtration steps, Protein A affinity chromatography, or anion exchange chromatography in flow-through mode, amino acid substitutions during lead optimization are less likely to have significant effects on the process performance. Thus, the developed in silico workflow supports one of the most development-intensive unit operations in our DSP platform. Future work should investigate how the identified correlations integrate into a holistic CMC developability assessment combining upstream, downstream, and formulation parameters.

The results in Section 3.2 confirmed a relationship between mAb structure and adsorption model parameters. Due to the semimechanistic nature of the commonly applied SMA adsorption model, an interpretation of model parameters is challenging, especially for multidomain molecules such as mAbs. The multicomponent SMA adsorption model (Brooks & Cramer, 1992) is an extension of the stoichiometric displacement concept developed by Boardman and Partridge (1955). Here, the characteristic charge describes multipoint binding of proteins on charged surfaces. In Section 3.2, the introduction of two additional charges per mAb could not increase the characteristic charge parameters of M1 and M2 in a magnitude that describes the shift in retention time. When comparing the constant $v_i$ parameters to constant pI values and protein net charges in Table 2, the characteristic charge can be assumed to describe the average number of positive patches on the protein surface interacting with the resin. In contrast to the characteristic charge, the equilibrium constant $k_{eq,i}$ was significantly increased by the introduction of positively charged groups within the adsorption-mediating region on the protein surface. Therefore, $k_{eq,i}$ may define the strength of the anisotropic adsorption reaction, depending on positive patches in mAb CDR. Substitution of the tryptophan residue in M2 reduced the steric shielding parameter $\sigma_i$. The reduction of $\sigma_i$ could have been caused by a combination of two effects. First, the conformational change of the H-CDR3 could have reduced the number of ligands blocked by the protein. Additionally, it has been observed that the steric shielding parameter can also describe repulsive effects on the resin surface (Ladiwala et al., 2005). Thus, the substitution of the aromatic tryptophan residue could have influenced hydrophobic interactions with the resin backbone leading to a reduced $\sigma_{M2}$ compared with $\sigma_{WT}$.

The knowledge gained on structural dependencies of model parameters could support the selection of plausible boundary conditions for model parameter estimation, which is crucial for avoiding local minima (Rischawy et al., 2019). Despite the influence of amino acid substitutions on adsorption model parameters, the data set is still limited to three variants of a monoclonal antibody. When increasing size and structural heterogeneity of the mAb data set, the found correlations could enable QSPR modeling for the prediction of SMA parameters. Conventional QSPR approaches for developability assessment correlate structural properties with specific performance indicators or quality attributes of the biopharmaceutical (Jetha et al., 2018; Sankar, Hoi, et al., 2018). A structure-based prediction of

adsorption model parameters could lead to a full digital representation of the unit operation enabling the simulation of an unlimited number of process conditions before material for wet-lab CMC activities is available.

## 5 | CONCLUSION

Our results demonstrate that sequence optimization of mAb candidates can influence downstream processing. Single amino acid substitutions in the CDR had a significant impact on retention volumes and elution profiles during preparative CEX chromatography. The findings enable a relative classification of mAb candidates in weak, medium, and strong adsorption to CEX media based on the number of positively charged amino acid side chains in the CDR. Substitution of tryptophan with lysine destabilized the H-CDR3 loop conformation, leading to an increased charge heterogeneity and broadened elution profiles in CEX chromatography. The identified relationship between mAb primary structure and CMC properties may support the selection of mAb candidates that integrate into common downstream platforms. Furthermore, a structure-based estimation of mAb elution behavior in CEX chromatography could be used to plan initial experiments during early-phase DSP development. Effects of amino acid substitutions on semimechanistic adsorption model parameters underline the possibility of building QSPR models that support the calibration of mechanistic chromatography models. Our results could promote a paradigm shift in DSP development from a strictly generic platform process to a more flexible process design driven by the structural characteristics of the mAb.

### CONFLICT OF INTERESTS

The authors declare that there are no conflict of interests.

### AUTHOR CONTRIBUTIONS

David Saleh, Rudger Hess, Michelle Ahlers-Hesse, Federico Rischawy, Gang Wang, Simon Kluters, contributed to the experimental design, data acquisition, and modeling. Nicole Beckert, Markus Schönberger, Joschka Bauer, Michaela Blech, designed, expressed, and purified the antibody variants. David Saleh, Rudger Hess, Federico Rischawy, Gang Wang, Simon Kluters, Joey Studts, Jürgen Hubbuch, wrote, edited, and discussed the manuscript.

### ORCID

David Saleh ![ORCID] http://orcid.org/0000-0002-1212-3679
Simon Kluters ![ORCID] https://orcid.org/0000-0002-3619-6821

## REFERENCES

Bailly, M., Mieczkowski, C., Juan, V., Metwally, E., Tomazela, D., Baker, J., Uchida, M., Kofman, E., Raoufi, F., & Motlagh, S. (2020). Predicting antibody developability profiles through early stage discovery screening. *mAbs*, *12*, 1.

Banerjee, S., Parimal, S., & Cramer, S. M. (2017). A molecular modeling based method to predict elution behavior and binding patches of proteins in multimodal chromatography. *Journal of Chromatography A*, *1511*, 45–58.

Bauer, J., Mathias, S., Kube, S., Otte, K., Garidel, P., Gamer, M., Blech, M., Fischer, S., & Karow-Zwick, A. R. (2020). Rational optimization of a monoclonal antibody improves the aggregation propensity and enhances the CMC properties along the entire pharmaceutical process chain. *mAbs*, *12*, 1787121.

Baumann, P., Hahn, T., & Hubbuch, J. (2015). High-throughput micro-scale cultivations and chromatography modeling: Powerful tools for integrated process development. *Biotechnology and Bioengineering*, *112*(10), 2123–2133.

Benner, S. W., Welsh, J. P., Rauscher, M. A., & Pollard, J. M. (2019). Prediction of lab and manufacturing scale chromatography performance using mini-columns and mechanistic modeling. *Journal of Chromatography A*, *1593*, 54–62.

Boardman, N., & Partridge, S. (1955). Separation of neutral proteins on ion-exchange resins. *Biochemical Journal*, *59*(4), 543–552.

Borg, N., Brodsky, Y., Moscariello, J., Vunnum, S., Vedantham, G., Westerberg, K., & Nilsson, B. (2014). Modeling and robust pooling design of a preparative cation-exchange chromatography step for purification of monoclonal antibody monomer from aggregates. *Journal of Chromatography A*, *1359*, 170–181.

Briskot, T., Stückler, F., Wittkopp, F., Williams, C., Yang, J., Konrad, S., Doninger, K., Griesbach, J., Bennecke, M., & Hepbildikler, S. (2019). Prediction uncertainty assessment of chromatography models using Bayesian inference. *Journal of Chromatography A*, *1587*, 101–110.

Brooks, C. A., & Cramer, S. M. (1992). Steric mass-action ion exchange: Displacement profiles and induced salt gradients. *AIChE Journal*, *38*(12), 1969–1978.

Close, E. J., Salm, J. R., Bracewell, D. G., & Sorensen, E. (2014). A model based approach for identifying robust operating conditions for industrial chromatography with process variability. *Chemical Engineering Science*, *116*, 284–295.

Dismer, F., & Hubbuch, J. (2010). 3D structure-based protein retention prediction for ion-exchange chromatography. *Journal of Chromatography A*, *1217*(8), 1343–1353.

Farid, S. S., Baron, M., Stamatis, C., Nie, W., & Coffman, J. (2020). Benchmarking biopharmaceutical process development and manufacturing cost contributions to R&D. *mAbs*, *12*(1), 1754999.

Freed, A. S., Garde, S., & Cramer, S. M. (2011). Molecular simulations of multimodal ligand–protein binding: Elucidation of binding sites and correlation with experiments. *The Journal of Physical Chemistry B*, *115*(45), 13320–13327.

Gudhka, R. B., Bilodeau, C. L., McCallum, S. A., McCoy, M. A., Roush, D. J., Snyder, M. A., & Cramer, S. M. (2020). Identification of preferred multimodal ligand-binding regions on IgG1 FC using nuclear magnetic resonance and molecular dynamics simulations. *Biotechnology and Bioengineering*, *118*, 809–822.

Guiochon, G., Felinger, A., Shirazi, D. G., & Katt, A. M. (2006). Transfer phenomena in chromatography. In: G. Guiochon (Ed.), *Fundamentals of preparative and nonlinear chromatography* (pp. 221–279). Academic Press.

Hahn, T., Baumann, P., Huuk, T., Heuveline, V., & Hubbuch, J. (2016). UV absorption-based inverse modeling of protein chromatography. *Engineering in Life Sciences*, *16*(2), 99–106.

Hahn, T., Huuk, T., Osberghaus, A., Doninger, K., Nath, S., Hepbildikler, S., Heuveline, V., & Hubbuch, J. (2016). Calibration-free inverse modeling of ion-exchange chromatography in industrial antibody purification. *Engineering in Life Sciences*, *16*(2), 107–113.

Hahn, T., Sommer, A., Osberghaus, A., Heuveline, V., & Hubbuch, J. (2014). Adjoint-based estimation and optimization for column liquid chromatography models. *Computers & Chemical Engineering*, *64*, 41–54.

Hunt, S., Larsen, T., & Todd, R. J. (2017). Modeling preparative cation exchange chromatography of monoclonal antibodies. In A. Staby & S. Ahuja (Eds.), *Preparative chromatography for separation of proteins*. John Wiley & Sons, Inc.

Huuk, T. C., Briskot, T., Hahn, T., & Hubbuch, J. (2016). A versatile noninvasive method for adsorber quantification in batch and column chromatography based on the ionic capacity. *Biotechnology Progress*, *32*(3), 666–677.

Huuk, T. C., Hahn, T., Osberghaus, A., & Hubbuch, J. (2014). Model-based integrated optimization and evaluation of a multi-step ion exchange chromatography. *Separation and Purification Technology*, *136*, 207–222.

Ishihara, T., Kadoya, T., Yoshida, H., Tamada, T., & Yamamoto, S. (2005). Rational methods for predicting human monoclonal antibodies retention in protein A affinity chromatography and cation exchange chromatography. *Journal of Chromatography A*, *1093*(1), 126–138.

Jakobsson, N., Degerman, M., Stenborg, E., & Nilsson, B. (2007). Model based robustness analysis of an ion-exchange chromatography step. *Journal of Chromatography A*, *1138*(1), 109–119.

Jetha, A., Thorsteinson, N., Jmeian, Y., Jeganathan, A., Giblin, P., & Fransson, J. (2018). Homology modeling and structure-based design improve hydrophobic interaction chromatography behavior of integrin binding antibodies. *mAbs*, *10*, 890–900.

Kaplon, H., Muralidharan, M., Schneider, Z., & Reichert, J. M. (2020). Antibodies to watch in 2020. *mAbs*, *12*(1), 1703531.

Kaplon, H., & Reichert, J. M. (2019). Antibodies to watch in 2019. *mAbs*, *11*(2), 219–238.

Kittelmann, J., Lang, K. M. H., Ottens, M., & Hubbuch, J. (2017a). An orientation sensitive approach in biomolecule interaction quantitative structure–activity relationship modeling and its application in ion-exchange chromatography. *Journal of Chromatography A*, *1482*, 48–56.

Kittelmann, J., Lang, K. M. H., Ottens, M., & Hubbuch, J. (2017b). Orientation of monoclonal antibodies in ion-exchange chromatography: A predictive quantitative structure–activity relationship modeling approach. *Journal of Chromatography A*, *1510*(suppl C), 33–39.

Kumar, S., Roffi, K., Tomar, D. S., Cirelli, D., Luksha, N., Meyer, D., Mitchell, J., Allen, M. J., & Li, L. (2018). Rational optimization of a monoclonal antibody for simultaneous improvements in its solution properties and biological activity. *Protein Engineering, Design and Selection*, *31*(7–8), 313–325.

Ladiwala, A., Rege, K., Breneman, C. M., & Cramer, S. M. (2005). A priori prediction of adsorption isotherm parameters and chromatographic behavior in ion-exchange systems. *Proceedings of the National Academy of Sciences of the United States of America*, *102*(33), 11710–11715.

Lan, W., Valente, J. J., Ilott, A., Chennamsetty, N., Liu, Z., Rizzo, J. M., Yamniuk, A. P., Qiu, D., Shackman, H. M., & Bolgar, M. S. (2020). Investigation of anomalous charge variant profile reveals discrete pH-dependent conformations and conformation-dependent charge states within the CDR3 loop of a therapeutic mAb. *mAbs*, *12*, 1763138.

Lang, K. M., Kittelmann, J., Dürr, C., Osberghaus, A., & Hubbuch, J. (2015). A comprehensive molecular dynamics approach to protein retention modeling in ion exchange chromatography. *Journal of Chromatography A*, *1381*, 184–193.

Liu, H., Gaza-Bulseco, G., Faldu, D., Chumsae, C., & Sun, J. (2008). Heterogeneity of monoclonal antibodies. *Journal of Pharmaceutical Sciences*, 97(7), 2426–2447.

Liu, H. F., Ma, J., Winter, C., & Bayer, R. (2010). Recovery and purification process development for monoclonal antibody production. *mAbs*, 2(5), 480–499.

Liu, H. F., McCooey, B., Duarte, T., Myers, D. E., Hudson, T., Amanullah, A., van Reis, R., & Kelley, B. D. (2011). Exploration of overloaded cation exchange chromatography for monoclonal antibody purification. *Journal of Chromatography A*, 1218(39), 6943–6952.

Mazza, C., Sukumar, N., Breneman, C., & Cramer, S. (2001). Prediction of protein retention in ion-exchange systems using molecular descriptors obtained from crystal structure. *Analytical Chemistry*, 73(22), 5457–5461.

Mollerup, J. M., Hansen, T. B., Kidal, S., Sejergaard, L., & Staby, A. (2007). Development, modelling, optimisation and scale-up of chromatographic purification of a therapeutic protein. *Fluid Phase Equilibria*, 261(1), 133–139.

Mollerup, J. M., Hansen, T. B., Kidal, S., & Staby, A. (2008). Quality by design—Thermodynamic modelling of chromatographic separation of proteins. *Journal of Chromatography A*, 1177(2), 200–206.

Müller-Späth, T., Aumann, L., Melter, L., Ströhlein, G., & Morbidelli, M. (2008). Chromatographic separation of three monoclonal antibody variants using multicolumn countercurrent solvent gradient purification (MCSGP). *Biotechnology and Bioengineering*, 100(6), 1166–1177.

Olsson, M. H., Søndergaard, C. R., Rostkowski, M., & Jensen, J. H. (2011). PROPKA3: Consistent treatment of internal and surface residues in empirical p$K_a$ predictions. *Journal of Chemical Theory and Computation*, 7(2), 525–537.

Osberghaus, A., Hepbildikler, S., Nath, S., Haindl, M., von Lieres, E., & Hubbuch, J. (2012). Determination of parameters for the steric mass action model—A comparison between two approaches. *Journal of Chromatography A*, 1233, 54–65.

Rischawy, F., Saleh, D., Hahn, T., Oelmeier, S., Spitz, J., & Kluters, S. (2019). Good modeling practice for industrial chromatography: Mechanistic modeling of ion exchange chromatography of a bispecific antibody. *Computers & Chemical Engineering*, 130, 106532.

Robinson, J., Roush, D., & Cramer, S. (2018). Domain contributions to antibody retention in multimodal chromatography systems. *Journal of Chromatography A*, 1563, 89–98.

Robinson, J., Roush, D., & Cramer, S. M. (2020). The effect of pH on antibody retention in multimodal cation exchange chromatographic systems. *Journal of Chromatography A*, 1617, 460838.

Robinson, J. R., Karkov, H. S., Woo, J. A., Krogh, B. O., & Cramer, S. M. (2017). QSAR models for prediction of chromatographic behavior of homologous Fab variants. *Biotechnology and Bioengineering*, 114(6), 1231–1240.

Rodrigues, A. E. (1997). Permeable packings and perfusion chromatography in protein separation. *Journal of Chromatography, B: Biomedical Sciences and Applications*, 699(1–2), 47–61.

Roos, K., Wu, C., Damm, W., Reboul, M., Stevenson, J. M., Lu, C., Dahlgren, M. K., Mondal, S., Chen, W., & Wang, L. (2019). OPLS3e: Extending force field coverage for drug-like small molecules. *Journal of Chemical Theory and Computation*, 15(3), 1863–1874.

Rüdt, M., Gillet, F., Heege, S., Hitzler, J., Kalbfuss, B., & Guélat, B. (2015). Combined Yamamoto approach for simultaneous estimation of adsorption isotherm and kinetic parameters in ion-exchange chromatography. *Journal of Chromatography A*, 1413, 68–76.

Saleh, D., Wang, G., Müller, B., Rischawy, F., Kluters, S., Studts, J., & Hubbuch, J. (2020). Straightforward method for calibration of mechanistic cation exchange chromatography models for industrial applications. *Biotechnology Progress*, 36, e2984.

Sankar, K., Hoi, K. H., Yin, Y., Ramachandran, P., Andersen, N., Hilderbrand, A., McDonald, P., Spiess, C., & Zhang, Q. (2018). Prediction of methionine oxidation risk in monoclonal antibodies using a machine learning method, 10, 1281–1290.

Sankar, K., Krystek, Jr, S. R., Carl, S. M., Day, T., & Maier, J. K. (2018). AggScore: Prediction of aggregation-prone regions in proteins based on the distribution of surface patches. *Proteins: Structure, Function, and Bioinformatics*, 86(11), 1147–1156.

Seeliger, D., Schulz, P., Litzenburger, T., Spitz, J., Hoerer, S., Blech, M., Enenkel, B., Studts, J. M., Garidel, P., & Karow, A. R. (2015). Boosting antibody developability through rational sequence optimization. *mAbs*, 7, 505–515.

Shukla, A. A., Hubbard, B., Tressel, T., Guhan, S., & Low, D. (2007). Downstream processing of monoclonal antibodies—Application of platform approaches. *Journal of Chromatography B*, 848(1), 28–39.

van der Kant, R., Bauer, J., Karow-Zwick, A. R., Kube, S., Garidel, P., Blech, M., Rousseau, F., & Schymkowitz, J. (2019). Adaption of human antibody λ and κ light chain architectures to CDR repertoires. *Protein Engineering, Design and Selection*, 32(3), 109–127.

van der Kant, R., Karow-Zwick, A. R., Van Durme, J., Blech, M., Gallardo, R., Seeliger, D., Aßfalg, K., Baatsen, P., Compernolle, G., & Gils, A. (2017). Prediction and reduction of the aggregation of monoclonal antibodies. *Journal of Molecular Biology*, 429(8), 1244–1261.

Wang, G., Briskot, T., Hahn, T., Baumann, P., & Hubbuch, J. (2017). Root cause investigation of deviations in protein chromatography based on mechanistic models and artificial neural networks. *Journal of Chromatography A*, 1515, 146–153.

Woo, J., Parimal, S., Brown, M. R., Heden, R., & Cramer, S. M. (2015). The effect of geometrical presentation of multimodal cation-exchange ligands on selective recognition of hydrophobic regions on protein surfaces. *Journal of Chromatography A*, 1412, 33–42.

Yamamoto, S., Nakanishi, K., & Matsuno, R. (1988). *Ion-exchange chromatography of proteins*. CRC Press.

Yamamoto, S., Nomura, M., & Sano, Y. (1987). Resolution of proteins in linear gradient elution ion-exchange and hydrophobic interaction chromatography. *Journal of Chromatography A*, 409, 101–110.

Zhou, J., Tsao, H.-K., Sheng, Y.-J., & Jiang, S. (2004). Monte Carlo simulations of antibody adsorption and orientation on charged surfaces. *The Journal of Chemical Physics*, 121(2), 1050–1057.

Zhu, K., & Day, T. (2013). Ab initio structure prediction of the antibody hypervariable H3 loop. *Proteins: Structure, Function, and Bioinformatics*, 81(6), 1081–1089.

Zhu, K., Day, T., Warshaviak, D., Murrett, C., Friesner, R., & Pearlman, D. (2014). Antibody structure determination using a combination of homology modeling, energy-based refinement, and loop prediction. *Proteins: Structure, Function, and Bioinformatics*, 82(8), 1646–1655.